



## Research article

## Preparation and characterization of polyacrylic acid-hydroxyapatite nanocomposite by microwave-assisted synthesis method



Sevgi Sözügeçer, Nursel Pekel Bayramgil\*

Department of Chemistry, Faculty of Science, Hacettepe University, 06800, Beytepe-Ankara, Turkey

## ARTICLE INFO

## Keywords:

Hydroxyapatite  
Microwave heating  
Nanoparticles  
Polyacrylic acid

## ABSTRACT

Polyacrylic acid, polyalkenoic acids in general, form the liquid ionomer phase of glass ionomer cements, which are frequently used in root restorations in dentistry. It is possible to obtain these ionomers with a fast, energy-efficient, high reaction efficiency and a clean method with microwave irradiation method. In this study, polyacrylic acid and its composite with nano HAp have been synthesized by microwave (MW) irradiation. The two-process parameters that were tested are MW intensity and reaction time. The polymerization was carried out at 110 °C up to 40 min and yield over 92% was produced in 30 min. The average molar mass of PAA was found as 11960 Da using a high-resolution mass spectrometer (TOF-MS). On the other hand, hydroxyapatite (HAp) nanoparticles have been prepared via the sol-gel procedure using potassium dihydrogen phosphate and calcium nitrate tetrahydrate as the precursors for phosphorus and calcium, respectively. XRD, EDS analysis revealed that the particles contain calcium deficient hydroxyapatite  $(Ca_{10-x}(HPO_4)_x(PO_4)_{6-x}(OH)_{2-x})$  (HAp) crystals with beta-TCP phase. Morphological observation by SEM measurement proved that the crystal particles of the HAp are very regular and granular, and their size is 25–45 nm in the longitudinal section. These particles were used in composite preparation with PAA. The yield of the composite obtained by heating at 500 W, 30 min was found to be 90%. From the FTIR and  $^1H$ -NMR results, it was observed that there was not only a physical but also an electrostatic interaction between HAp and PAA. The thermal behavior of PAA and its composite with nano HAp were determined by the thermogravimetric analyzer (TGA). The results showed that anhydride formation or decarboxylation occurred at a lower temperature, confirming the interaction between PAA and HAp. The polymerization rate is much faster with microwave heating than conventional heating. Microwave irradiation enables rapid energy transfer and high-energy efficiency, hence, a faster reaction rate.

## 1. Introduction

Amalgam, composite resin, and glass ionomer types of cement are used as restorative materials to protect and strengthen healthy dental tissues in routine clinical applications of modern dentistry. Adjustable chemical composition and powder-liquid ratios of glass ionomer types of cement allow them to have a wider range of uses. Although they have a more aesthetic appearance than amalgam materials, the glass ionomer type of cement is not as successful as composite resins in terms of application [1, 2, 3, 4, 5]. However, thanks to their potential anti-cariogenic properties due to fluorine release, their biocompatibility, and chemical adaptability to the dental tissue, glass ionomer types of cement have become special materials. On the other hand, their weak mechanical properties limit their use. To avoid this problem, a second phase such as ceramic, glass fiber, or metal is added to the cement.

Hydroxyapatite (HAp) is calcium phosphate, the building block of human hard tissues in terms of morphology and chemical composition. Its most important feature is its high stability in the presence of physiological conditions such as temperature, pH, and chemical composition in body fluids compared to other calcium phosphates. It has superior properties such as biocompatible, bioactive, osteoconductive, and non-toxic, as well as no inflammatory effect. However, due to the low adhesion strength and also the brittle structure on the surface it diffuses, this hard structure can undergo fracture even under a very low stretching force. Besides, HAp does not have sufficient strength and durability for use in load carrying applications. The use of nano-scale particulate materials has been considered to overcome this problem, to ensure stronger adhesion, and to obtain superior mechanical properties [6, 7]. Nano hydroxyapatite (nano HAp) is a very attention-drawing biomaterial for use in prosthetic applications because of its similarity to human hard

\* Corresponding author.

E-mail address: [nursel@hacettepe.edu.tr](mailto:nursel@hacettepe.edu.tr) (N.P. Bayramgil).

tissue in terms of size, crystallinity, and chemical composition. Bone and tooth enamel are largely composed of a form of this mineral. HAp has been widely used for dental applications due to its excellent biocompatibility since human teeth are natural composites that contain nano HAp rods arranged in lamellae and bound to collagen. There are several ways to prepare nano HAp synthetically, such as co-precipitation, sol-gel process, spray pyrolysis, hydrothermal synthesis, emulsion processing, and mechano-chemical method. Among these, the sol-gel method provides the ability to form nanocrystalline powders, bulk amorphous monolithic solids, and thin films with molecular mixing at low processing temperatures. The sol-gel processing technique, which provides greater control over the formation of certain phases and the purity of the formed phases and provides lower processing temperatures, has not been extensively applied to the formation of hydroxyapatite powders, films, or bulk forms [8, 9].

The properties of the glass ionomer type of cement are directly affected by the type of polymer. In the structure of glass ionomer cement, polyalkenoic acids such as acrylic acid, maleic acid, itaconic acid, butane dicarboxylic acid, vinyl phosphoric acid, and copolymers of acrylic acid can be included [10]. Polyvinylphosphoric acid is not preferred because it has limited use only to adjust the powder-liquid ratio [2]. On the other hand, most intensive studies are done with polyacrylic acid. Polyacrylic acid can bind to calcium and form hydrogen bonds with organic polymers such as collagen [11]. Polyacrylic cement can also be attached to hydroxyapatite contained in enamel and dentin, as well as their biocompatibility and good physical properties. When examining the polymer-nano HAp composites, adhesion of polymer matrix to the dental fillers has primary importance on the composite properties. Since hydrophilicity or polarity of the filler directly affects the interfacial bonding between the filler and polymer matrix, the polymers having functional groups improve the adhesion. Moreover, the high molecular weight of the fillers fosters the mechanical strength of cement while increasing viscosity, making it difficult to mix [1]. Therefore, it is important to select a reasonable molecular weight to provide stability in dental practice.

Since Gedye and Giguere/Majetich [12, 13] first published the use of microwave irradiation to carry out organic chemical transformations, numerous articles have been published in this field by taking advantage of short reaction times, increased product yields, enhanced product purities, and reduced side reactions due to microwave heating. Due to its unique properties such as high efficiency, low energy consumption, high speed, high flexibility, high purity, homogeneity, and short reaction time, the heating process using a microwave as an energy source is widely used in almost all chemical processes, especially for solving in analytical chemistry, synthesis in organic chemistry and recently in polymerization. New materials (composites, hydrogels, etc.) are synthesized by microwave-assisted polymerization [14, 15]. The reaction occurs rapidly in microwave heating. Because MW energy penetrates not only to the outer surface of the reaction system but also to the inside. Since the heating in conventional heating systems only affects the outer surface, it is inefficient in terms of the heat reaching and reacting to the reactants remaining inside. MW energy permits the reaction to take place homogeneously by penetrating inside and outside of the reaction, so the reaction takes place in a shorter time. Also, MW does not require post-reaction heating or cooling processes, thus enabling more efficient use of time [16]. The numbers of reactions were reported as products proved to be faster with the use of microwave irradiation as a heat source compared to conventional heating. Today, microwave-assisted synthesis is preferred in multistep synthesis, medicinal chemistry, polymer synthesis, material sciences, nanotechnological applications, and biochemical processes [17, 18, 19]. By this convenience, the product obtained by microwave-assisted synthesis might be cheaper and reproducible.

Glass ionomer cements are indispensable in dental applications. It is used for adhesive cement, base material, restoration of root surface caries, tunnel cavity restorations, and aesthetic purposes. When glass (containing silica, alumina, fluoride) and ionomer (polyacrylic acid)

react, the acid dissolves the glass and releases Ca, Al, Na, and F ions. PAA then forms chains and cross-links with Ca ions. Adhesion of glass ionomer cements can be improved with short-term phosphoric acid or polyacrylic acid applied to the cavity. The carboxyl groups of PAA and Ca ions in the hydroxyapatite in enamel and dentin form chelate. The main reason for planning this study is to prepare HAp-containing polyacrylic acid material that will help renew bone tissue in dental applications, especially in repairing root surface caries. HAp was synthesized in nanoscale because it was aimed to create more contact points with the dental tissue by increasing the surface area. The composite material was obtained by microwave heating, which is a synthesis method that is fast, clean, energy-efficient, high yield, and does not cause any negative effects on the physical properties of the final product, instead of conventional heating. Polyacrylic acid, which is the main component of dental filling material and glass ionomer cement, was synthesized by microwave irradiation. Nano hydroxyapatite particles were obtained by the sol-gel method and nanocomposites were prepared by mixing with polyacrylic acid under optimum synthesis conditions. The effects of microwave irradiation time and microwave energy on polymerization were investigated. The polymer and its nanocomposite were characterized by the FT-IR, <sup>1</sup>H-NMR, SEM, EDS, XRD, TGA, and TOF-MS methods.

## 2. Materials and methods

Potassium dihydrogen phosphate (KDP), calcium nitrate tetrahydrate (CNT), ammonia (NH<sub>3</sub>), acrylic acid (AA), benzene (as a solvent), N, N-methylene bisacrylamide (MBAAm) (crosslinker), and n-heptane were purchased from Sigma-Aldrich (USA). 2,2'-Azobis(2-methylpropionitrile) (AIBN) as initiator, purchased from Merck (Darmstadt, Germany), was recrystallized twice from methanol before use.

0.6 M KDP and 1.0 M CNT solutions were prepared with distilled water and used as starting materials. CNT solution was added dropwise to the KDP solution while stirring. To adjust pH = 10, the NH<sub>3</sub> solution was added. While adding the NH<sub>3</sub> solution, white precipitates came out at the bottom of the beaker. This precipitated solution was stirred for 1 h and kept at room temperature for 24 h. The mixture was filtrated and washed with distilled water to eliminate by-products (KOH- potassium hydroxide, NH<sub>4</sub>NO<sub>3</sub>-ammonium nitrate). The obtained precipitate was dried at 40 °C for 24 h in a dry oven. The dried powder was calcined at 600 °C for 1 h with the electrical furnace.

Based on the studies of Mishra et al. [20] and Jovanovic et al. [21], a certain amount of AIBN, benzene, and AA in Table 1 were added to a test vial of working volume V = 10 mL. The vial was then sealed using a rubber cap and purged with high-purity (>99.999%) N<sub>2</sub> flow for 5 min to remove the moisture and oxygen. Then, it was placed in the microwave equipment (Milestone-RotaPREP, Figure 1) and irradiated at 110 °C. All the microwave-assisted reactions were carried out in closed Teflon vessels at variable microwave power and irradiation time. After the irradiation was complete, the as-polymerized product was precipitated in n-heptane following dissolution in benzene to remove unreacted monomer, waste solvent, and oligomeric products. White powder polymer was dried in the oven and stored at 40 °C.

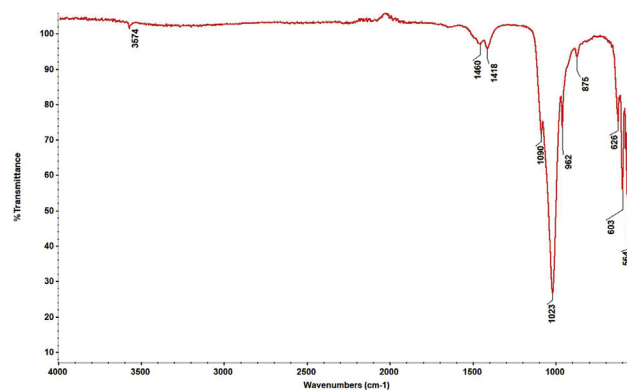
Composites were synthesized by using certain amounts of materials given in Table 2. AIBN and MBAAm were dissolved in benzene. Then AA and nano HAp were added to the solution in a test vial and deoxygenated with N<sub>2</sub> bubbling. All the other procedures were the same as that of the microwave-assisted synthesis of PAA.

The FT-IR spectra of AA/nano HAp composites were taken by Thermo Scientific Nicolet iS10 FT-IR spectrophotometer in the region of 4000–400 cm<sup>-1</sup>. Before the analyses, samples were ground into fine particles, mixed with KBr by grinding, and compressed into a pellet. The spectra were obtained through 10 scanning procedures at 4 cm<sup>-1</sup> resolution.

The <sup>1</sup>H-NMR spectra of AA and its polymer were recorded using DMSO-d<sub>6</sub> solvent on Bruker DPX-400 FT-NMR Spectrometer, operated at 400 MHz.

**Table 1.** Polymerization parameters for acrylic acid.

Sample #	AIBN (mole %)	AA (mole %)	Benzene (mL)	Input Power (Watt)	Reaction time (min)	Yield %
1	0.2	99.8	4.0	500	10	15
2	0.2	99.8	4.0	500	40	28
3	0.4	99.6	4.0	300	20	13
4	0.4	99.6	4.0	300	30	34
5	0.4	99.6	4.0	500	7	53
6	0.4	99.6	4.0	500	10	60
7	0.5	99.5	4.0	150	20	23
8	0.5	99.5	4.0	300	20	43
9	0.5	99.5	4.0	300	30	56
10	0.5	99.5	4.0	400	20	72
11	0.5	99.5	4.0	500	7	49
12	0.5	99.5	4.0	500	10	63
13	0.5	99.5	4.0	500	20	87
14	0.5	99.5	4.0	500	30	92

**Figure 1.** Milestone-RotaPREP equipment for microwave heating.**Figure 2.** FT-IR spectrum of synthesized nano HAp.

XRD patterns of nano HAp and its AA composites were obtained at room temperature on a Cu K $\alpha$  radiation source using the PANalytical Empyrean X-ray diffractometer in the  $2\theta$  range  $5^\circ$ – $70^\circ$  with a scanning speed of  $2^\circ$ /min.

Scanning electron micrographs of nano HAp and its composite with AA were taken using SEM (Carl Zeiss Supra 40VP model). The samples were coated with gold to ensure conductivity and mounted in a sample holder. The photomicrograph of samples was taken at an accelerating voltage at 20 kV at different magnifications. Inorganic particle distributions in nanocomposite hydrogels were determined by an EDS detector.

TGA analyses were performed with Thermo Plus EVO simultaneous TGA/DSC calorimeter (Rigaku, Japan) in the temperature range of (20–480 °C) at a heating rate of 10 °C per minute in the N<sub>2</sub> atmosphere.

Waters, Synapt G1 model high-resolution mass spectrometer (TOF-MS ES) were used to calculate the molecular weight of PAA.

### 3. Results and discussion

In this study, which investigates the filling of polyacrylic acid with nano HAp to increase the mechanical strength of glass ionomer cement used as tooth filling material, FT-IR spectrum was taken to describe the functional groups of nano HAp obtained by the sol-gel method. In the spectrum seen in Figure 2, the functional groups corresponding to the significant bands of HAp are given in Table 3.

The morphology of synthesized nano HAp was evaluated by Scanning Electron Microscopy (SEM), and its composition (Ca/P ratio) was determined by Energy Dispersive X-ray spectroscopy (EDS). SEM image was presented in Figure 3. Nano HAp was observed in a granular structure similar to flower seed and particle size was calculated in the range of 25–50 nm. The EDS analysis, in Figure 4, revealed that nano HAp particles consisted of calcium, phosphorus, and oxygen atoms. According to

**Table 2.** Polymerization parameters for PAA-nano HAp composites.

Sample #	AIBN (mole %)	MBAAm (mole %)	AA (mole %)	Benzene (mL)	Nano HAp (g)	Input Power (Watt)	Reaction time (min)	Yield %
1	0.5	0.1	99.4	4.0	0.02	300	20	46
2	0.5	0.1	99.4	4.0	0.02	300	30	61
3	0.5	0.1	99.4	4.0	0.02	500	7	54
4	0.5	0.1	99.4	4.0	0.02	500	20	78
5	0.5	0.1	99.4	4.0	0.02	500	30	90

**Table 3.** Functional groups that correspond to important bands in the FT-IR spectrum of nano HAp.

Wavenumbers (cm <sup>-1</sup> )	Functional groups	
564–603	PO <sub>4</sub> <sup>3-</sup>	(asymmetrical bending vibration)
626	OH <sup>-</sup>	(structural)
875	HPO <sub>4</sub> <sup>2-</sup>	(stretching mode)
962	PO <sub>4</sub> <sup>3-</sup>	(symmetrical stretching vibration)
1023–1090	PO <sub>4</sub> <sup>3-</sup>	(asymmetrical stretching vibration)
1418	CO <sub>3</sub> <sup>2-</sup>	(symmetrical stretching vibration)
1460	CO <sub>3</sub> <sup>2-</sup>	(asymmetrical stretching vibration)
3574	OH <sup>-</sup>	(symmetrical stretching vibration)

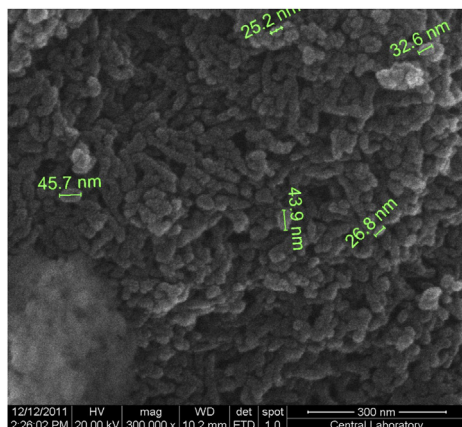
the elemental analysis, the Ca/P ratio was found as 1.52. In the light of the literature [22], we think that the corresponding calcium phosphate form to this ratio is mainly beta-TCP but calcium-deficient HAp. Another significant finding that reinforces this argument is that we saw the band belonging to the CO<sub>3</sub><sup>2-</sup> groups and the HPO<sub>4</sub><sup>2-</sup> group at 875 cm<sup>-1</sup> in the FT-IR spectrum caused by the impurities inherent in the reactants added to the synthesis medium. The CO<sub>3</sub><sup>2-</sup> groups may be substituted with the OH<sup>-</sup> group or the PO<sub>4</sub><sup>3-</sup> group. Thus, calcium-deficient HAp structures are obtained [23].

The formation of nano-hydroxyapatite was also characterized by XRD analysis. In Figure 5, the XRD peaks of synthesized hydroxyapatite and its standard JCPDS 9-432 card were given together for comparison. The main reflections indexed as (002), (211), (300) and (202) were observed at  $2\theta = 26.09273, 32.13266, 33.18308$  and  $34.33854^\circ$ , respectively. When the characteristic structures of the peaks are examined, sharp, high peaks generally indicate that the structure is highly crystalline, but wide peaks show that the crystal size is quite small. It was also found that the calcium phosphate form obtained in the experiment was pure HAp when compared with the card, but it turned out to be calcium deficient HAp as revealed by the FT-IR and EDS measurements. Using XRD patterns, the crystallite size can be estimated based on the Scherrer formula (Eqn 1). However, since a particle may contain more than one crystallite, an average crystallite size may be obtained.

Scherrer equation:

$$L = \frac{K \cdot \lambda}{B \cdot \cos \theta} \quad (\text{Eqn 1})$$

$L$  is the average thickness in a vertical direction of the crystal face;  $K$  is a Scherrer constant or shape factor (generally assumed as 0.9 for spherical particles);  $B$  is the full width at half the maximum (FWHM) in radians of the X-ray diffraction peak;  $\lambda$  is the wavelength of X-ray source (0.154 nm for Cu/K $\alpha$ );  $\theta$  is the Bragg's angle (deg).

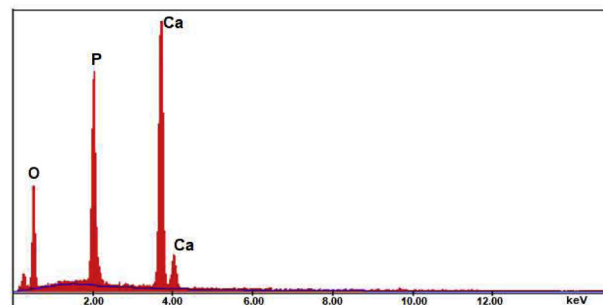
**Figure 3.** SEM image of nano HAp particles.

The crystallite size was calculated as 13 nm with the Scherrer formula. This value is approximately the same as the size calculated by the cross-sectional view on SEM images and it is possible to say that the obtained calcium deficient HAp has a small particle size.

Since microwave is recognized as an effective and non-ionizing electromagnetic energy source, it draws attention as an environmentally friendly and reliable method for multistage, ring-opening, and radical polymerization processes. In this study, composites containing PAA and nano HAp were prepared using a microwave. The curves in Figures 6, 7, and 8 present the effects of initiator amount, microwave energy intensity, and reaction time on the polymerization of acrylic acid.

In radical polymerization, there are two basic reactions in the initial step: firstly, the initiator being broken down to form radicals; and secondly, these radicals are added into the monomer molecules in the medium to initiate the propagation step. According to the ideal polymerization kinetics, an increase in the initiator concentration increases the polymerization rate and leads to a decrease in molecular weight. Since the radicals formed by the thermal decomposition of the initiator trigger polymerizations from different centers, the rate increases but small chain polymers are formed at the end of the reaction. As shown in Figure 6, yield % increased with increasing AIBN concentration. Figure 7 presents the effect of MW intensity on the yield %. When the intensity of MW increases, the initiator which starts to disintegrate immediately with the increasing reaction temperature causes an increase in the polymerization rate due to the reaction between the formed radicals and the monomers, thus increasing the yield. The MW irradiation time is another important factor affecting the polymerization kinetics and yield %. Prolonged irradiation time results in increased polymer yield. Furthermore, the polymer yield % observed at a lower MW intensity, together with the increased MW energy density, leads to a shortening of the polymerization time while increasing the polymerization temperature. For example, the polymer yield % observed at 300 W, 20 min was 43%, while under 500 W MW intensity this ratio was reached in the first 7 minutes (Figure 8, Table 1).

When microwave heating is applied under isothermal conditions, thermally unstable species such as monomer, initiator, crosslinker, and

**Figure 4.** EDS spectrum for synthesized nano HAp.

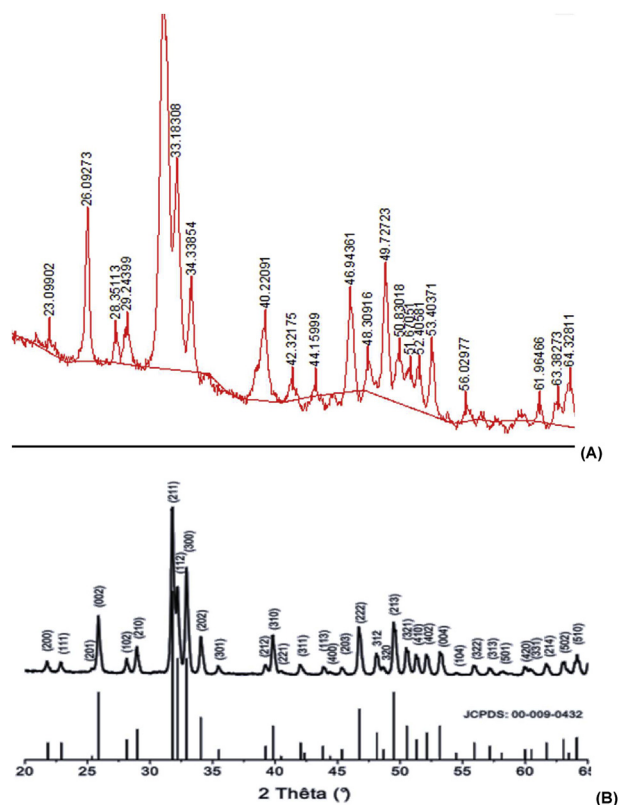


Figure 5. XRD patterns for synthesized nano Hap (A) and its standard JCPDS card (B).

macroradical absorb the suddenly generated microwave energy. Microwave energy absorption increases the connatural energy of the species. The thermally nonequibrated distribution of connatural energy of the species has higher values than the equilibrated Maxwell-Boltzman thermal distribution of the energy of the species. This is because the activation energy of PAA formation is inversely proportional to the connatural energy of the species. As a result, as the connatural energy of the initiator molecules increases, the activation energy decreases and the initiator molecules rapidly dissociate. This is the reason why the initial rate and polymer yield are significantly increased [20].

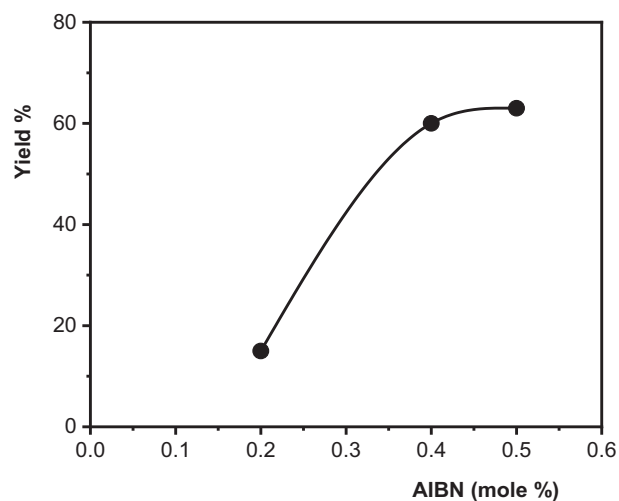


Figure 6. Plot of yield % of PAA formation vs. mole % of AIBN (MW intensity: 500 W, time: 10 min).

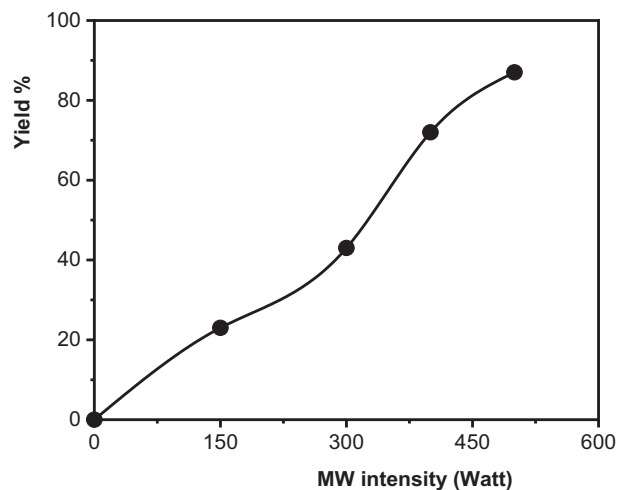


Figure 7. Plot of yield % of PAA formation vs. microwave irradiation energy (AIBN mole %: 0.5, Time: 20 min).

There are many studies on the use of microwave radiation in dentistry. However, most of these studies are related to the use of dental materials/devices for disinfection. However, the widespread use of microwave irradiation to polymerize acrylic resin, to dry gypsum products and investment materials, and as a post-polymerization treatment to reduce residual monomer content and cytotoxicity of polymerized acrylic resins has also been accepted [24]. According to Azzarri et al. [25], optimizing the residual monomer level and achieving better mechanical properties while keeping cytotoxicity low is possible with proper MW power selection and resin curing time. Machado et al. [26] studied heat curing of acrylic resin by using both conventional (74 °C, 9 h) and microwave irradiation (500 W, 3 min). They stated that the relationship between polymerization using microwave irradiation and mechanical polishing indicated lower percent solubility, indicating lower residue release. Some applications of microwave energy in the field of dentistry are the disinfection of removable prostheses and the use of this disinfection method in the treatment of patients with oral candidiasis. The microbiological efficacy of microwave irradiation has been proven by studies and this efficacy is directly dependent on the irradiation protocol adopted. Parameters to be considered when defining a microwave irradiation protocol; the exposure time, the strength of the microwave energy, the type of material, the medium into which the material is immersed, and the type of microorganisms that colonize the material.

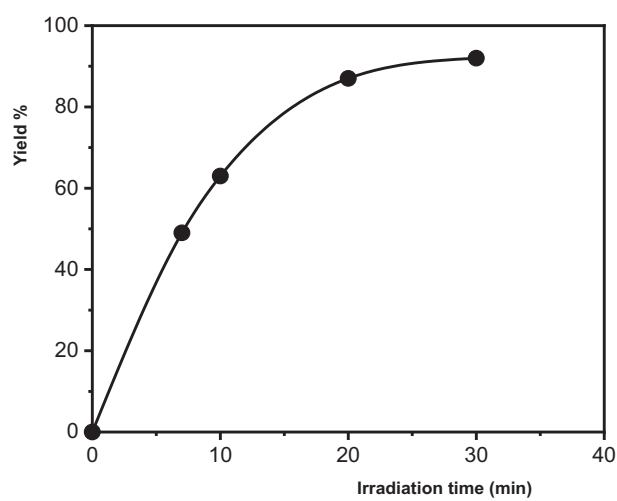


Figure 8. Plot of yield % of PAA formation vs. irradiation time (AIBN mole %: 0.5, MW intensity: 500 W).

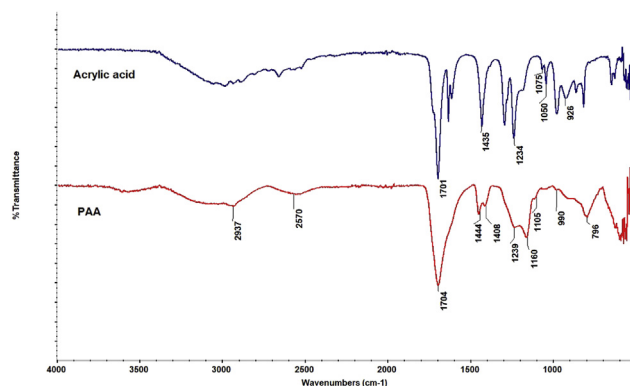


Figure 9. FTIR spectra of acrylic acid and its polymer synthesized under microwave heating.

There's logical prove to back the adequacy of microwave irradiation in avoiding cross-infection and treating denture stomatitis. A few irradiation schemes have been portrayed and discussed, and the microbiological effectiveness of microwave energy has been illustrated [27].

Figure 9 shows the FTIR spectra of the acrylic acid subject to the MW heating (500 W, 30 min) in the initial concentration of 0.5% mole of AIBN (taking into account the polymer yield, MW intensity, and irradiation time) and the obtained polymer. A broad peak at 3250–3000  $\text{cm}^{-1}$  belongs to stretching and out-of-plane bending of  $-\text{OH}$ . Medium peaks at 2900 and 1408–1444  $\text{cm}^{-1}$  belong to asymmetric stretching and bending vibration respectively of  $-\text{CH}_2-$  groups. A band around 1700  $\text{cm}^{-1}$  belongs to the stretching of carbonyl of  $-\text{COOH}$  groups. The bands near 1230  $\text{cm}^{-1}$  are attributed to the in-plane deformation of  $-\text{OH}$  groups. It is important to note that the band at 1050  $\text{cm}^{-1}$  belonging to  $-\text{C}=\text{C}-$  of acrylic acid is not included in the polyacrylic acid spectrum. This observation is indicative of the successful conversion of acrylic acid to polyacrylic acid.

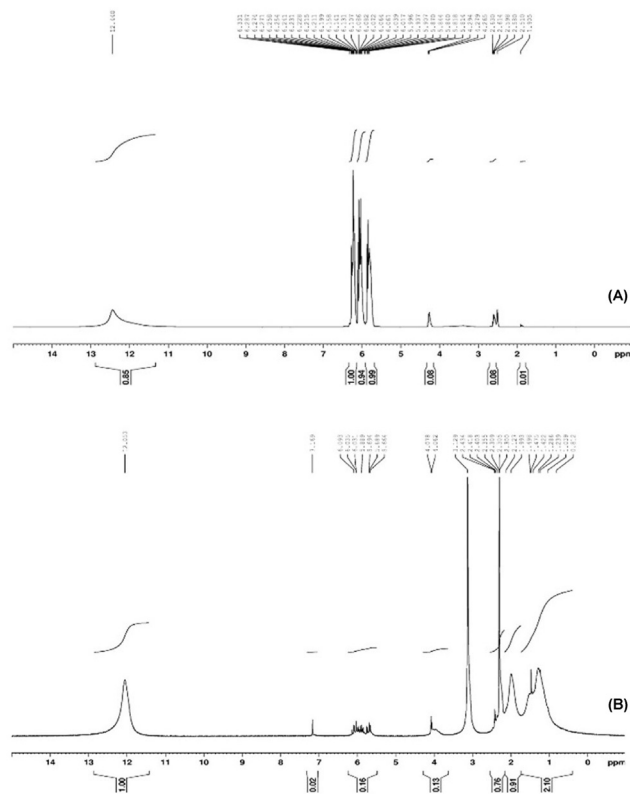


Figure 10.  $^1\text{H}$ -NMR spectra of acrylic acid (A) and polyacrylic acid (B).

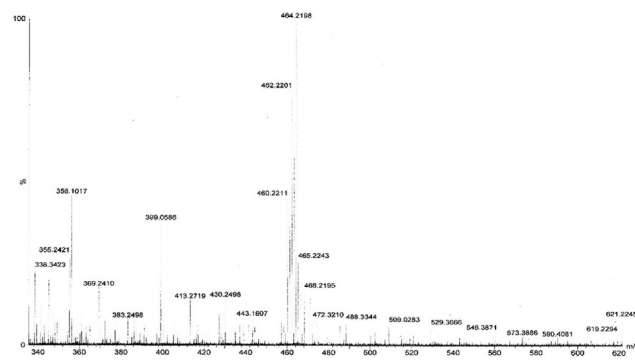


Figure 11. TOF-MS result for PAA.

Figure 10 indicates the  $^1\text{H}$ -NMR spectra of acrylic acid and its polymer. The spectrum of pure AA (Figure 10 A) consists of three quadruplets centered at 6.25 ppm (cis proton), 5.87 ppm (germinal proton), and 5.82 ppm (trans proton) [28]. After polymerization,  $^1\text{H}$ -NMR spectra (Figure 10 B) showed peaks of  $-\text{CH}_2$  protons in the polyacrylic acid chain in the range of 1.3–1.8 ppm, and peaks of  $-\text{CH}$  protons in 2.4 ppm. It was also found that impurities were resulting from the solvent  $\text{DMSO}-d_6$  used. The acid proton showed itself at 12 ppm. The fact that peaks in acrylic acid are still present in the polyacrylic acid spectrum, even at low intensity, indicates that we cannot completely remove the residual monomer from the polymer after washing.

A high-resolution mass spectrum of PAA was presented in Figure 11. The average molecular mass value for PAA was found to be 11960 Da.

In the second stage of the study, PAA composites containing HAP were prepared by MW irradiation. Here, in dentistry, it is aimed to observe the synergistic effect of adding nano HAP particles with the increased surface area into glass ionomer cements to be applied to dental tissue, with the idea of strengthening the connection to bone tissue, especially in healing root surface caries. Nano HAP can help tissue healing as well as promote new dental tissue by realizing multi-point bonding with bone tissue. Since the MW irradiation method offers clean, fast, high-efficiency products, composites were obtained in this method. The characterization results for the PAA-nano HAP composite are given below, in comparison with that of pure PAA, respectively. The composites were obtained by subjecting the mixtures (prepared by adding 0.02 g of nano HAP to the reaction vessel consisting of 0.5% mole AIBN, 0.1% mole of MBAAm, 99.4% mole AA), taking into account the characterization results presented for pure PAA, to MW heating at 300 W and 500 W for 7, 20 and 30 minutes. The yield of the composite obtained by heating at 500 W, 30 minutes was found to be 90%.

The FTIR spectra obtained for the structural analysis of this composite and nano HAP are given in Figure 12. The peaks observed in the FTIR spectrum for the composite were evaluated taking into account the

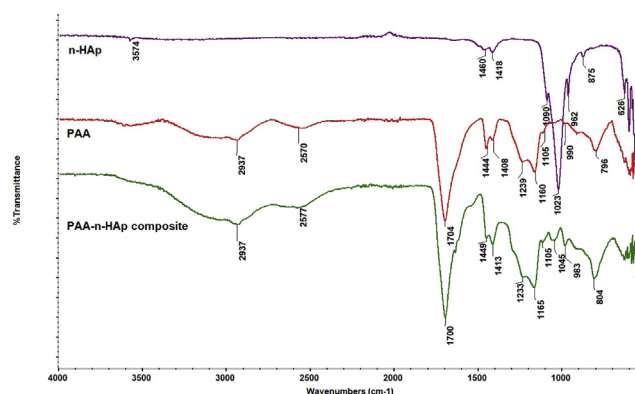


Figure 12. FTIR spectra of nano HAP, polyacrylic acid, and its composite.

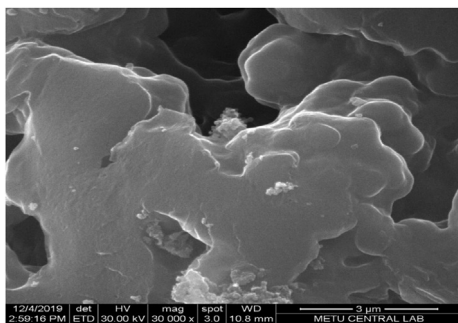


Figure 13. SEM image for PAA-nano HAp composite.

previously detailed peaks for nano HAp and pure PAA (see Table 3 and Figure 9). The fact that the asymmetric stretching vibration of the  $\text{PO}_4^{3-}$  group, which was absent in the pure PAA but present in nano HAp at  $1023\text{ cm}^{-1}$ , was included in the composite's FTIR spectrum at  $1045\text{ cm}^{-1}$ , and that the symmetric stretching vibration of the  $\text{PO}_4^{3-}$  group at  $962\text{ cm}^{-1}$  was at  $983\text{ cm}^{-1}$ , suggests an association between the  $-\text{COOH}$  group of acrylic acid and  $\text{PO}_4^{3-}$  group of HAp. The following events also draw attention: the overlap between the asymmetric stretching and bending vibration of the  $-\text{CH}_2-$  groups of pure PAA at  $1408$  and  $1444\text{ cm}^{-1}$  along the main chain and the  $\text{CO}_3^{2-}$  asymmetric and symmetric stretching vibrations of the nano HAp approximately within the same range, as well as changing relative intensity ratios of the dual-band within said range along the FTIR spectrum of the composite upon a potential interaction.

These observed changes indicate that nano HAp and pure PAA are not merely a physical mixture but also carry possible intrinsic electrostatic interactions.

Figure 13 shows an SEM image of the polyacrylic acid - nano HAp composite. Granular structures in the SEM image obtained for nano HAp were replaced by very smooth and homogeneous structures in the composite structure. As mentioned earlier, possible electrostatic interactions between the  $\text{PO}_4^{3-}$  group of HAp and the  $-\text{COOH}$  group of acrylic acid are the leading causes of this distribution.

The composition (Ca/P ratio) of the PAA-nano HAp composite was again determined from the EDS result (Figure 14). Considering the composite composition, the Ca/P ratio was found to be 1.18. This result is lower than the value found for pure HAp and corresponds to amorphous HAp [22]. Therefore, it may be possible to say that the crystal structure of HAp is rearranged due to its interaction with PAA.

The crystal structure of the PAA-nano HAp composite was characterized by XRD analysis. In Figure 15, the diffractogram is characterized by an intense and broad signal at the angle of  $2\theta = 26.6^\circ$  and a shoulder at  $2\theta = 38.7^\circ$ , in accord with other works [29]. The basic peaks observed in pure HAp structure were shifted in the composite structure at  $2\theta = 31.70, 32.84, \text{ and } 34.38^\circ$ . This observation demonstrates the presence of

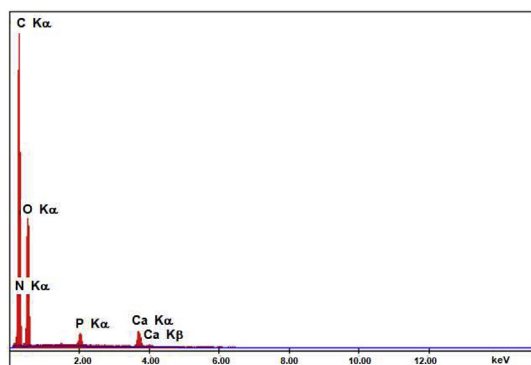


Figure 14. EDS spectrum for PAA-nano HAp composite.

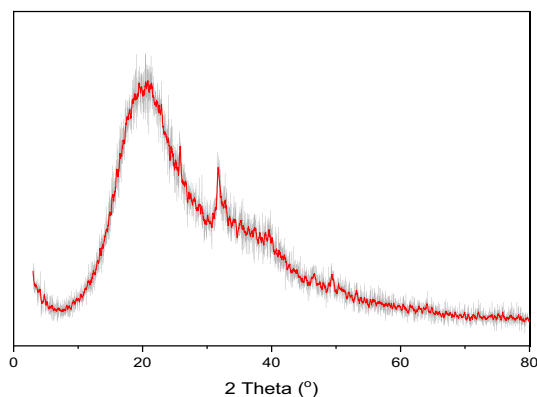


Figure 15. XRD patterns of PAA-nano HAp composite.

the interaction between the  $-\text{COOH}$  group of acrylic acid and  $\text{PO}_4^{3-}$  and possible  $\text{CO}_3^{2-}$  groups in the HAp structure.

Finally, thermal analyses of the polymer and composite obtained in this study were performed using TGA. Figure 16 shows the TGA and derivative TGA curves of both pure PAA and its composite with nano HAp. Thermal decomposition curves of acrylic acid consist of two parts. The first disruption attributed to the destruction of side groups in PAA leading to decarboxylation or anhydride formation ( $\sim 30\%$  mass loss at  $288^\circ\text{C}$ ), and the second disruption resulted from the main chain scission ( $\sim 45\%$  mass loss at  $345^\circ\text{C}$ ). In the *der.*TGA curve obtained for the composite, acrylic acid main chain degradation was observed at  $344^\circ\text{C}$ , while degradation indicating the formation of anhydride or decarboxylation was observed at lower temperature:  $247^\circ\text{C}$ . The reason for this observation can be explained as follows: While repetitive  $-\text{COOH}$  groups along the PAA main chain lead to the formation of anhydride by the separation of  $\text{CO}_2$  among themselves, possible interactions of  $-\text{COOH}$  groups with  $\text{PO}_4^{3-}$ ,  $\text{HPO}_4^{2-}$  and  $\text{OH}^-$  groups (which are added together with nano HAp to composite structure) prevent the anhydride formation but result in new complex formations.

Based on all the analyses presented so far, the possible interaction/reaction between the carboxylate groups of PAA and calcium ions of nano HAp is indicated in the following scheme (Figure 17). Given that polyacrylic acids well adhere to dental tissue, this case is arisen from the ion-binding potential of HAp. Where water is present, via  $-\text{COOH}$  groups, PAA attacks HAp and causes the release of calcium cation; this process also results in the formation of inter-intramolecular salt bridges.

#### 4. Conclusion

The preparation of polymer/HAp composite materials is of awesome intrigued to dental applications other than the improvement of

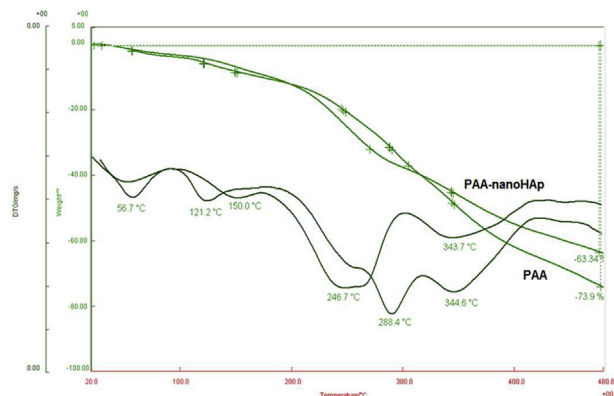


Figure 16. TGA and *der.*TGA curves for PAA and its composite with nano HAp.

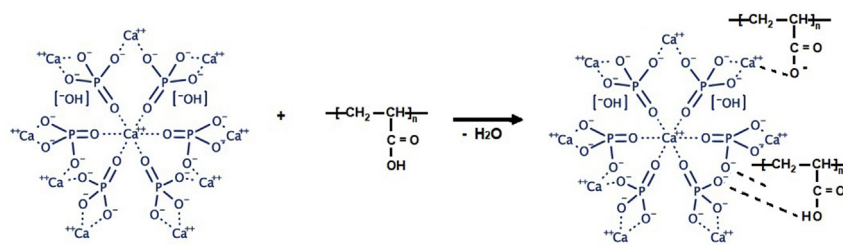


Figure 17. The possible interaction between the carboxylate groups of PAA and calcium ions of HAP.

biomaterials suitable to repair the skeletal system. The inorganic component of bone tissue, maybe the foremost imperative biological composite, is constituted of hydroxyapatite crystals inserted in a collagenous network. One of the main advantages of polymer/HAP composites concerning HAP biomaterials is the possibility to modulate biodegradability, bioactivity, and mechanical properties through variations in composition. In this study, polyacrylic acid and polyacrylic acid/nano-sized HAP composites were prepared by using the microwave heating method. The effects of microwave irradiation time and microwave energy on polymerization were investigated. 92 and 90 % polymer yields for pure PAA and its nano HAP composite, respectively were recorded at 500 W, 30 min. All FT-IR, SEM, XRD results showed that there may be more than electrostatic interaction between the calcium and phosphate ions of HAP and the carboxyl groups of PAA. In this study, it was demonstrated that HAP polymer composites to be used as glass ionomer cement (GIC) can be obtained by microwave heating in a shorter time with higher efficiency.

## Declarations

### Author contribution statement

Sevgi Sözügeçer: Performed the experiments; Analyzed and interpreted the data.

Nursel Pekel Bayramgil: Conceived and designed the experiments; Analyzed and interpreted the data; Contributed reagents, materials, analysis tools or data; Wrote the paper.

### Funding statement

This research did not receive any specific grant from funding agencies in the public, commercial, or not-for-profit sectors.

### Data availability statement

The authors are unable or have chosen not to specify which data has been used.

### Declaration of interests statement

The authors declare no conflict of interest.

### Additional information

No additional information is available for this paper.

## References

- [1] U. Lohbauer, Dental glass ionomer cements as permanent filling materials? - properties, limitations and future trends, *Materials* 3 (1) (2010) 76–96.
- [2] S.K. Sidhu, J.W. Nicholson, A review of glass-ionomer cements for clinical dentistry, *J. Funct. Biomater.* 7 (3) (2016) E16.
- [3] J.O. Burgess, D. Cakir, Material Selection for Direct Posterior Restoratives, PennWell Publications, 2013. [http://www.ineedce.com/courses/2067/pdf/1108ce\\_i\\_dentsply\\_restoratives.pdf](http://www.ineedce.com/courses/2067/pdf/1108ce_i_dentsply_restoratives.pdf).
- [4] H. Torabzadeh, A. Ghasemi, S. Shakeri, A.A. Baghban, S. Razmavar, Effect of powder/liquid ratio of glass ionomer cements on flexural and shear bond strengths to dentin, *Braz. J. Oral Sci.* 10 (3) (2011) 204–207. ISSN: 0949-2321, WOS: 000215874400457.
- [5] K.J. Anusavice, Challenges to the development of esthetic alternatives to dental amalgam in a dental researcher center, *Trans. Acad. Dent. Mater.* 9 (1996) 25–50.
- [6] E. Pepla, L.K. Besharat, G. Palaia, G. Tenore, G. Migliau, Nano-hydroxyapatite and its applications in preventive, restorative and regenerative dentistry: a review of literature, *Ann. Stomatol.* 5 (3) (2014) 108–114. PMID: PMC4252862.
- [7] H. Zhou, J. Lee, Nanoscale hydroxyapatite particles for bone tissue engineering, *Acta Biomater.* 7 (7) (2011) 2769–2781.
- [8] P.W. Brown, Hydroxyapatite-polymer composites, *Phosphorus, Sulfur Silicon Relat. Elem.* 144 (1) (1999) 57–60.
- [9] A.K. Gaharwar, S.A. Dammou, J.M. Canter, C.J. Wu, G. Schmidt, Highly extensible, tough, and elastomeric nanocomposite hydrogels from poly(ethylene glycol) and hydroxyapatite nanoparticles, *Biomacromolecules* 12 (5) (2011) 1641–1650.
- [10] S. Crisp S, B.E. Kent, B.G. Lewis, A.J. Ferner, A.D. Wilson, Glass ionomer cement formulations. II. The synthesis of novel polycarboxylic acids, *J. Dent. Res.* 59 (6) (1980) 1055–1063.
- [11] R.G. Craig, J.M. Powers, *Restorative Dental Materials*, eleventh ed., Mosby, London, UK, 2002.
- [12] R. Gedye, R. Smith, K. Westaway, H. Ali, L. Baldisera, et al., The use of microwave ovens for rapid organic synthesis, *Tetrahedron Lett.* 27 (3) (1986) 279–282.
- [13] R.J. Giguere, T.L. Bray, S.M. Duncan, G. Majetich, Application of commercial microwave ovens to organic synthesis, *Tetrahedron Lett.* 27 (41) (1986) 4945–4948.
- [14] Y. Chen, D. Ni, X. Yang, C. Liu, J. Yin, K. Cai, Microwave-assisted synthesis of honeycomb like hierarchical spherical Zn-doped Ni-MOF as a high-performance battery-type supercapacitor electrode material, *Electrochim. Acta* 278 (2018) 114–123.
- [15] Y. Qi, Y. Cao, X. Meng, K. Yu, W. Si, W. Lei, Q. Hao, J. Li, F. Wang, Microwave-assisted synthesis of a polypyrrole/graphene composite using a pyrrole-induced graphene oxide hydrogel for the selective determination of dihydroxybenzenes, *Chem. Select* 3 (27) (2018) 7713–7717.
- [16] J. Zhao, W. Yan, Chapter 8 - microwave-assisted inorganic syntheses, in: R. Xu, W. Pang, Q. Huo (Eds.), *Modern Inorganic Synthetic Chemistry*, Elsevier, 2011, pp. 173–195.
- [17] D. Bogdal, P. Penczek, J. Pielichowski, A. Prociak, Microwave assisted synthesis, crosslinking, and processing of polymeric materials, *Adv. Polym. Sci.* 163 (2003) 194–263.
- [18] G.A. Tompsett, W.C. Conner, K.S. Yngvesson, Microwave synthesis of nanoporous materials, *ChemPhysChem* 7 (2) (2006) 296–319.
- [19] W.N. Sandoval, V. Pham, E.S. Ingle, P.S. Liu, J. R Lill, Applications of microwave-assisted proteomics in biotechnology, *Comb. Chem. High Throughput Screen.* 10 (9) (2007) 751–765.
- [20] M.K. Mishra, S.N. Bhadani, Free-radical polymerization of acrylic acid in benzene, *J. Macromol. Sci. Part A - Chem.* 22 (2) (1985) 235–242.
- [21] J. Jovanovic, B. Adnadjevic, Influence of microwave heating on the kinetic of acrylic acid polymerization and crosslinking, *J. Appl. Polym. Sci.* 116 (1) (2010) 55–63.
- [22] L. Berzina-Cimdina, N. Borodajenko, Research of calcium phosphates using fourier transform infrared spectroscopy, in: T. Theophile (Ed.), *Infrared Spectroscopy - Materials Science, Engineering and Technology*, InTech, 2012, pp. 123–148.
- [23] Y. Sekine, R. Motokawa, N. Kozai, et al., Calcium-deficient hydroxyapatite as a potential sorbent for strontium, *Sci. Rep.* 7 (2017) 2064.
- [24] C. Vergani, D.G. Ribeiro, L.N. Dovigo, P.V. Sanita, A.C. Pavarina, Microwave Assisted Disinfection Method in Dentistry, *Microwave Heating*, Usha Chandra, IntechOpen, 2011.
- [25] M.J. Azzarri, M.S. Cortizo, J.L. Alessandrini, Effect of the curing conditions on the properties of an acrylic denture base resin microwave-polymerised, *J. Dent.* 31 (2003) 463–468. ISSN 0300-5712.
- [26] C. Machado, C.M. Rizzatti-Barbosa, M. Gabriotti, F. Joia, M.C. Ribeiro, R.L.S. Sous, Influence of mechanical and chemical polishing in the solubility of acrylic resins polymerized by microwave irradiation and conventional water bath, *Dent. Mater.* 20 (2004) 565–569. ISSN 0109-5641.
- [27] P.V. Sanita, C.E. Vergani, E.T. Giampaolo, A.C. Pavarina, A.L. Machado, Growth of Candida species on complete dentures: effect of microwave disinfection, *Mycoses* 52 (2009) 154–160. ISSN 0933-7407.
- [28] A.C. Lira, M. Flores, R. Arroyo, U. Caldiño, Optical spectroscopy of Er<sup>3+</sup> ions in poly(acrylic acid), *Opt. Mater.* 28 (10) (2006) 1171–1177.
- [29] S. Sun, X. Chen, J. Liu, J. Yan, Y. Fang, A novel two-component physical gel based on interaction between poly(acrylic acid) and 6-deoxy-6-amino-β-cyclodextrin, *Polym. Eng. Sci.* 49 (1) (2009) 99–103.